NATIONAL AERONAUTICS AND SPACE ADMINISTRATION U.S.A.

FLIGHT-MEASURED BASE PRESSURE COEFFICIENTS FOR THICK BOUNDARY-LAYER FLOW OVER AN AFT-FACING STEP FOR MACH NUMBERS FROM 0.4 TO 2.5

by Sheryll A. Goecke

Flight Research Center
Edwards, Calif. 93523

1. Report No. TN D-7202	2. Government Accession No.	3. Recipient's Catalog No.
4. Title and Subtitle FLIGHT-MEASURED BASE PRESSURE COEFFICIENTS FOR THICK BOUNDARY-LAYER FLOW OVER AN AFT-FACING STEP FOR MACH NUMBERS FROM 0.4 TO 2.5		5. Report Date May 1973
		6. Performing Organization Code
7. Author(s) Sheryll A. Goecke		8. Performing Organization Report No. H-740
		10. Work Unit No. 501-06-08-00-24
9. Performing Organization Name and Address NASA Flight Research Center P. O. Box 273 Edwards, California 93523		11. Contract or Grant No.
		13. Type of Report and Period Covered Technical Note
12. Sponsoring Agency Name and Address National Aeronautics and Space Administration Washington, D. C. 20546		14. Sponsoring Agency Code

15. Supplementary Notes

16. Abstract

A 1.42-centimeter- (0.56-inch-) thick aft-facing step was located 15.9 meters (52.1 feet) from the leading edge of the left wing of an XB-70 airplane. A boundary-layer rake at a mirror location on the right wing was used to obtain local flow properties. Reynolds numbers were near 10^8, resulting in a relatively thick boundary layer. The momentum thickness ranged from slightly thinner to slightly thicker than the step height. Surface static pressures forward of the step were obtained for Mach numbers near 0.9, 1.5, 2.0, and 2.4. The data were compared with thin boundary-layer results from flight and wind-tunnel experiments and semiempirical relationships. Significant differences were found between the thick and the thin boundary-layer data.

17. Key Words (Suggested by Author(s)) Separated flow Base pressure	18. Distribution Statement Unclassified - Unlimited		
19. Security Classif. (of this report) Unclassified	20. Security Classif. (of this page) Unclassified	21. No. of Pages 32	22. Price* $3.00

FLIGHT-MEASURED BASE PRESSURE COEFFICIENTS FOR THICK

BOUNDARY-LAYER FLOW OVER AN AFT-FACING STEP FOR

MACH NUMBERS FROM 0.4 to 2.5

Sheryll A. Goecke
Flight Research Center

INTRODUCTION

The drag penalty resulting from blunt trailing edges, surface discontinuities along the trailing edges of panels, and other aft-facing discontinuities can add significantly to the total drag of an airplane. These drag penalties (base pressures) are difficult to predict; for example, the base pressure coefficient for the propulsion installation on the XB-70 airplane was about three times larger (more negative) than the predicted values at Mach numbers near 1.2 (ref. 1). Theoretical, wind-tunnel, and flight studies (refs. 2 to 11) have helped in the development of methods for predicting the base pressure on steps and wedges in thin boundary layers (momentum thickness of 0.38 centimeter (0.15 inch) or less). However, most aft-facing discontinuities on large subsonic and supersonic aircraft are immersed in thick boundary-layer flows for which little or no base pressure data are available.

The present study on the XB-70 airplane was initiated to determine the base pressure on an aft-facing discontinuity in the presence of a thick boundary layer. The large, relatively flat wing surfaces of the airplane provided an excellent surface on which to build an aft-facing step. Because of the long distance from the wing leading edge to the step, the aft-facing step was immersed in a thick (momentum thickness from 0.99 centimeter to 1.90 centimeters (0.40 inch to 0.74 inch)), quasi-two-dimensional boundary layer. Preliminary results are presented in reference 12. The static pressure was measured on the base surface for free-stream Mach numbers from 0.4 to 2.5. The surface static pressure profile in front of the step was obtained over much of this Mach number range. A boundary-layer rake at a mirror location on the right wing provided information for determining local viscous and boundary-layer-edge flow conditions.

The 1.42-centimeter (0.56-inch) step height is comparable to the step heights and trailing edge thicknesses used in earlier studies (refs. 5 to 9), but both the Reynolds number (near 10^8) and the momentum thickness of the present study are larger than in the previous studies. Consequently, the data of this experiment, which represent a real flight environment, extend available knowledge beyond the momentum-thickness-to-step-height ratio of most previous experiments into the range of values that large airplanes of the future will encounter. Also presented are the effects of the step on the surface pressure distribution immediately in front of the step and comparisons of the flight data with data from earlier studies.

SYMBOLS

Physical quantities in this report are given in the International System of Units (SI) and parenthetically in U.S. Customary Units. The measurements were taken in Customary Units. Factors relating the two systems are presented in reference 13.

c chord distance to step, m (ft)

c_f local skin friction coefficient, compressible

c_p' pressure recovery coefficient, $\dfrac{p_r - p_b}{0.7M_1^2 p_b}$

$c_{p,b}$ base pressure coefficient, $\dfrac{p_b - p_r}{0.7M^2 p_r}$

D drag, N (lb)

h step height (2h is equivalent to trailing edge thickness), cm (in.)

k Mach-number-dependent value (fig. 13)

M free-stream Mach number

M_1 Mach number in main stream where the static pressure is p_b

p static pressure, N/m^2 (lb/ft^2)

R Reynolds number, $\dfrac{\rho u c}{\mu}$

$S_{(\ )}$ standard deviation of subscripted variable

u velocity, m/sec (ft/sec)

u_τ frictional velocity just in front of step, $\left(\dfrac{\tau}{\rho_s}\right)^{1/2}$, m/sec (ft/sec)

x longitudinal distance from step (in front of step is negative), cm (in.)

y distance above surface (perpendicular to x), cm (in.)

| ΔD | drag increment, N (lb) |

ΔD drag increment, N (lb)

δ boundary-layer thickness, cm (in.)

θ momentum thickness, cm (in.)

μ absolute viscosity, $\dfrac{\text{kg-sec}}{\text{m}^2}\left(\dfrac{\text{lb-sec}}{\text{ft}^2}\right)$

ν kinematic viscosity, m^2/sec (ft^2/sec)

ρ density of fluid, $\dfrac{\text{kg-sec}^2}{\text{m}^4}\left(\dfrac{\text{lb-sec}^2}{\text{ft}^4}\right)$

τ skin frictional stress just in front of step, kg/m^2 (lb/ft^2)

Subscripts:

b   step face or base of aft-facing step

e   conditions at edge of boundary layer

l   limit condition

r   local reference

s   conditions based on surface temperature just in front of step

y   variation in y direction

∞ free stream

TEST CONFIGURATION

A two-view drawing of the XB-70 airplane is shown in figure 1. A description of the airplane and its physical characteristics are included in reference 14. The aft-facing step experiment was installed on the upper surface of the left wing, and the boundary-layer rake used to obtain the local flow properties was in a mirror location on the upper surface of the right wing.

The aft-facing step experiment required a wing surface contour change which covered an area 91.2 centimeters (35.9 inches) wide and 227.3 centimeters (89.5 inches) long. The modification consisted of constructing a ramp region, reference region, and recovery region (figs. 2(a) and 2(b)). The ramp region, which had a slope of 0° 33', provided a gradual transition for the flow from the wing surface to the height of the reference region. The surface of the reference region followed the surface contour of the adjacent wing and terminated with a right-angle

step down to the recovery region. The reference and recovery region surfaces were parallel to within 0°12'. The side edges of each of the three regions were faired onto the wing surface at an angle of approximately 45°. The step height of 1.42 centimeters (0.56 inch) was chosen so that the ratio of momentum thickness to step height, θ/h, was near 1.

The ramp and reference regions were built up with balsa wood. The balsa wood was then covered with a room-temperature-vulcanizing silicone rubber (RTV).[1] (See reference 15 for method of application.) The RTV was sanded and painted until the surface was aerodynamically smooth, that is, until the surface roughness was contained within the laminar sublayer and caused no increase in drag compared with a smooth wall. To keep the reattachment surface parallel to the reference region, RTV was applied to the recovery region surface 15.5 centimeters (6.1 inches) downstream of the step, which was considerably longer than the calculated reattachment length of 8.64 centimeters (3.4 inches).

The locations of the pressure orifices are shown in figure 3. The pressure measured from the orifice 31.0 centimeters (12.2 inches) in front of the step was used as the local reference pressure. The pressures from the three base orifices were manifolded to give an average base pressure measurement.

The surfaces of the reference and recovery regions were aerodynamically smooth and free of joints. All the orifices in the reference region were drilled normal to the surface in a machined and polished metal surface. The edges of the orifices were sharp (that is, free of observable radius) and free of burrs. All the joints near the step were carefully sealed to insure that base bleed did not exist.

The boundary-layer rake is shown in figure 4. Its dimensions are given in reference 16. The static-pressure orifice for the boundary-layer rake and the local static reference pressure orifice for the aft-facing step experiment were in mirror locations on the right and left wings, respectively. Both were 4.4 meters (14.3 feet) from the centerline of the fuselage and 15.6 meters (51.1 feet) aft of the wing leading edge.

INSTRUMENTATION

A 48-port multiplexing valve (Scanivalve) with a differential pressure transducer referenced to the local static reference pressure was used to measure the differential base pressure and static pressure in front of the base. The local static reference pressure was included in the pressure survey in front of the step; therefore the Scanivalve transducer was referenced to itself and took an "in-flight zero" with each complete cycle. The data from the Scanivalve were recorded on an onboard analog system. The local static reference pressure and the base pressure were also measured by individual differential pressure transducers. The differential transducer that measured the base pressure was referenced to the local static reference pressure. Thus, the differential base pressure was measured by two separate

---

[1]RTV, formally designated high temperature aerodynamic smoothing compound, was developed by North American-Rockwell Corp.

systems. The local static reference pressure transducer was referenced to the airplane reference pressure, that is, a plenum pressure obtained from static orifices on the nose boom. The airplane reference pressure was measured by a high-resolution absolute-pressure transducer which was kept in a carefully controlled temperature environment.

Free-stream Mach number was obtained from onboard sensor data and was corrected by using a calibration obtained from a combination of radar, radiosonde, and Pacer aircraft data. The nose boom and how the data were obtained and analyzed are described in reference 17. Angle of attack, angle of sideslip, and altitude, as well as airspeed, were obtained from sensors on the nose boom.

All the information used in this study except the Scanivalve data were recorded on an onboard digital sytem – a pulse code modulation (PCM) system. All records were synchronized by a time code generator.

A discussion of the instrumentation system for the boundary-layer rake and static orifice on the right wing can be found in reference 16.

ACCURACY

The standard deviations in the pressure ratios and the base pressure coefficients were calculated for two cases: (1) data obtained continuously through the entire flight, and (2) data obtained during periods of up to 6 minutes of steady-state flight. Only the Scanivalve data are considered for the steady-state case, even though data were also obtained with the individual differential pressure transducers during steady-state flight.

The standard deviations in the base pressure and the local reference pressure for the continuous data were $S_{p_b} = S_{p_r} = \pm368$ N/m^2 (±7.7 lb/ft^2). For the steady-state Scanivalve data, the values for the local static (or base) pressure and the local reference pressure were $S_p = S_{p_r} = \pm138$ N/m^2 (±2.9 lb/ft^2). The errors for the Scanivalve pressure data were smaller, primarily because (1) the Scanivalve transducer was referenced to its own reference pressure source for an interval during every cycle, thus, pressure differences could be determined which were free of bias; and (2) the data were obtained for several cycles, thus, an average value could be used. The standard deviation in Mach number obtained from reference 17 for Mach numbers between 1.4 and 2.5, for the altitudes of this experiment, was ±0.005 for both cases.

The standard deviations for the pressure ratios and the base pressure coefficients were found by using the following relationships, which were derived from equation (37) in reference 18:

$$S_{p/p_r} = \sqrt{\left(\frac{\partial\left(p/p_r\right)}{\partial p_r}\right)^2 \left(S_{p_r}\right)^2 + \left(\frac{\partial\left(p/p_r\right)}{\partial p}\right)^2 \left(S_p\right)^2}$$

5

and

$$S_{c_{p,b}} = \sqrt{\left(\frac{\partial c_{p,b}}{\partial p_b}\right)^2 \left(S_{p_b}\right)^2 + \left(\frac{\partial c_{p,b}}{\partial p_r}\right)^2 \left(S_{p_r}\right)^2 + \left(\frac{\partial c_{p,b}}{\partial M}\right)^2 \left(S_M\right)^2}$$

The term containing the standard deviation in Mach number was negligible in comparison with the other terms; after deleting it and simplifying, the final expressions for determining the standard deviations became

$$S_{p/p_r} = \frac{1}{p_r} \sqrt{\left(-p/p_r\right)^2 \left(S_{p_r}\right)^2 + \left(S_p\right)^2}$$

and

$$S_{c_{p,b}} = \frac{1}{0.7M^2 p_r} \sqrt{\left(S_{p_b}\right)^2 + \left(-p_b/p_r\right)^2 \left(S_{p_r}\right)^2}$$

The standard deviations for both cases are shown in the following table:

M	Continuous data		Steady-state data	
	S_{p_b/p_r}	$S_{c_{p,b}}$	S_{p/p_r}	$S_{c_{p,b}}$
1.5	±0.031	±0.020	±0.014	±0.013
2.0	±.037	±.018	±.024	±.013
2.4	±.068	±.018	±.035	±.012

Pressure lag was studied by comparing the continuous and the steady-state data. Lag effects were found to be noticeable only at Mach numbers between approximately 0.95 and 1.0, and thus did not influence the conclusions of this report.

TEST CONDITIONS

Free-stream Mach number, hereafter referred to as Mach number, ranged from 0.4 to 2.5 for the data of this experiment. The surface pressure profile in front of the step, the corresponding base pressure, the skin friction coefficient,[1] and the boundary-layer momentum thickness[2] were all obtained during steady-state flight.

It was assumed that turbulent flow began at the wing leading edge, because the step was far enough downstream that the transition location did not affect the data. Therefore the turbulent flow Reynolds number is based on the length of the chord from the leading edge to the step (15.9 meters (52.1 feet)).

Aircraft angle of attack and angle of sideslip varied respectively from $2.7°$ to $5.6°$ and $-0.5°$ to $0.7°$, with few exceptions, for the data presented.

RESULTS AND DISCUSSION

Surface Pressure Profile

Transonic and supersonic pressure profiles in front of the step are shown in figure 5. Each represents an average value obtained during steady-state flight conditions. The local pressures are normalized with respect to one of the surface pressures that was far enough upstream to be unaffected by the step, as indicated in the figure. The effect of the lower pressures from the base of the step in this thick boundary layer is propagated upstream from the step (or separation edge) for approximately four step heights. The influence of the lower pressure from the base of the step, beginning approximately four step heights ahead of the separation edge, appears as an expansion in the transonic case (M = 0.90), while in the supersonic cases a gentle compression appears first and is followed by an expansion.

In figure 6(a) the thin boundary-layer wind-tunnel data of reference 8 for M = 0.90 are compared with the M = 0.90 flight data of the present study. Because the transonic wind-tunnel pressure profiles of reference 8 are given as a pressure ratio with respect to the free-stream pressure, the transonic flight pressure ratios are also presented with respect to the free-stream pressure. The data show that the transonic pressure adjustments to base pressure, as a fluid element moves downstream, range from the gentle expansion of the flight pressure data and the more

---

[1]The skin-friction coefficient and boundary-layer profiles obtained on the XB-70 airplane are discussed in reference 16.

[2]The momentum thickness was calculated from boundary-layer-rake data using the relationship

$$\theta = \int_o^\delta \frac{\rho_y u_y}{\rho_e u_e}\left(1 - \frac{u_y}{u_e}\right)dy$$

abrupt expansion of the wedge pressure data of reference 8 to the unexpected compression of the step pressure data of reference 8.

In figure 6(b) the thin boundary-layer wind-tunnel data of reference 9 for M = 2.40 are compared with the flight data for similar Mach numbers. The upstream influence of the lower pressure on the base for the wind-tunnel data is less than one step height, and, as stated in reference 9, this indicates that the negative pressure gradient at separation does not propagate upstream as in the laminar case. However, the flight data seem sensitive to the effect for approximately four step heights upstream from the separation edge. That the effect is greater in a thick boundary layer is not unexpected, because the pressure influence of the step is transmitted upstream through the subsonic portion of the supersonic turbulent boundary layer. Since the boundary layer for the present study is approximately 20 times as thick as the boundary layer in reference 9, the subsonic portion would also be thicker. Consequently, the lower pressure caused by the step has a larger region in which to propagate forward.

Base Pressures

The ratio of base pressure to local reference pressure is presented as a function of Mach number in figure 7. The flight data were obtained from four flights during both the increasing and decreasing Mach number portions of the flight. Some of the data were for steady-state flight conditions which lasted up to 6 minutes.

The thin boundary-layer wind-tunnel data from reference 6 are for approximately the same θ/h as the thick boundary-layer flight data.[1] Agreement is good near M = 1.5, but near M = 2.4 the base pressure ratio for the wind-tunnel data is considerably higher (less drag) than for the flight data.

The variation in the base pressure ratio at given Mach numbers is examined in figures 8(a), 8(b), and 8(c). In these figures the base pressure ratios from the present study (thick boundary layer) and from references 3 to 7 and 10 (thin boundary layers) are plotted as a function of θ/h for Mach numbers near 1.5, 2.0, and 2.4. The trend of increasing base pressure ratio with increasing θ/h is observed at all three Mach numbers.

Data for base pressure ratios for θ/h near 1 are limited to the thick boundary-layer data of the present study, the thin boundary-layer data of reference 6, and the semiempirical estimate from reference 3. The plotted values from all three sources agree for Mach numbers near 1.5 (fig. 8(a)), but, as in figure 7, the base pressure ratio for the thin boundary-layer data is considerably higher than it is for the thick

---

[1]The thin boundary-layer data previously discussed herein were for boundary layers which were thin both in an absolute sense (momentum thickness of 0.38 centimeter (0.15 inch) or less) and in a relative sense (the step height was much larger than the momentum thickness). However, the data of reference 6 are for a boundary layer which is thin in an absolute sense but not in a relative sense; that is, the momentum thickness is the same order of magnitude as the step height or trailing edge thickness. Hereafter, the term "thin boundary layer" refers to boundary layers which are thin in an absolute sense; no distinction will be made concerning the relative sense.

boundary-layer flight data for Mach numbers near 2.4 (fig. 8(c)). The semi-empirical estimate from reference 3 tends to agree better with the thin boundary-layer data of reference 6 than with the thick boundary-layer flight data for Mach numbers near 2.4. At Mach numbers near 2.4, the values of θ/h for the flight data range from 0.8 to 1.3. These changes were related to changes in aircraft altitude and angle of attack.

Although presenting the results in terms of base pressure ratio clearly demonstrates the agreement or disagreement between data in this study and previous studies, it yields little direct information about the relative effects on drag. Therefore, the data of the present study are next presented as base pressure coefficients, which are related to drag more directly. In figure 9 the flight base pressure coefficients of the present study are compared with subsonic wind-tunnel data and with predicted subsonic and supersonic values. Several theories and semiempirical methods exist for predicting the supersonic base pressure in thin boundary-layer flows (for example, refs. 2 and 11); however, no theoretical or semiempirical base pressure prediction method was found for thick boundary-layer flows in any of the literature reviewed, which included references 19 and 20. Therefore, the predicted supersonic base pressure coefficients were calculated by using the data in figure 8 (open symbols) for the same θ/h values as the present flight data. At $M = 1.5$ agreement between the predicted values and the flight data was good, but at $M = 2.0$ the flight results were 20 percent more negative (corresponding to more drag) than predicted, and at $M = 2.4$ the flight results were 50 percent more negative than predicted.

Methods for predicting subsonic base pressures in thin boundary-layer flow are limited, and, as in the supersonic case, no theoretical method was found for thick boundary-layer flow in the literature reviewed, which included reference 20. However, the semiempirical method of Hoerner (ref. 21) provides realistic values for both the thin boundary-layer data of reference 8 and the thick boundary-layer flight data of the present study; in fact, the agreement between the flight data and the values predicted by using Hoerner's method is good. His method uses θ/h to account for the effects of boundary-layer thickness. The subsonic predictions in figure 9 were calculated by using the θ/h values of the present study and those of reference 8 in the following equation (from ch. 3, ref. 21):

$$c_{p,b} = \frac{-0.1}{\left(\dfrac{2\theta}{h}\right)^{1/3}}$$

The subsonic flight data for a thick boundary layer (θ/h near 1) have a less negative base pressure coefficient than the subsonic wind-tunnel data from reference 8 for a thin boundary layer ($\theta/h = 0.03$). This trend of more negative base pressure coefficient (more drag) with decreasing θ/h agrees with the trend shown by the supersonic data in figure 8. The subsonic flight data, as well as having a less negative base pressure coefficient than the data from reference 8, do not have the abrupt negative peak near $M = 1.1$ which is characteristic of thin boundary-layer data. Instead, the thick boundary layer seems to greatly moderate the transonic peak, so that the data gradually reach a maximum value between the Mach numbers of 1.3 and 1.5 before beginning the decrease that is characteristic of supersonic flow.

Comparison of Present Study With Generalized Correlation
Methods for Supersonic Mach Numbers

Correlating turbulent boundary-layer base pressure data for a relatively comprehensive range of Mach numbers and boundary-layer thicknesses has been attempted. Three approaches based on thin boundary-layer data are reported in references 3, 6, and 10. In this section, the thick boundary-layer data from the present study are compared with relationships developed by using these different correlation methods. The correlation parameter for each method is based primarily on Mach number.

The first generalized method was developed in reference 6. The method uses the concept of local similarity based on the law of the wall for turbulent boundary layers. The correlating parameter, c'_p, shown in figure 10, is a function of both Mach number and base pressure coefficient. Values of c'_p were calculated for the flight data of the present study using the relationship, from reference 6,

$$c'_p = \frac{p_r - p_b}{0.7M_1^2 p_b}$$

where M_1 is the Mach number in the main stream where the static pressure is p_b. Hastings (ref. 6) obtained a limiting value of c'_p in terms of $\frac{hu_\tau}{\nu_s}$ by examining his data and other thin boundary-layer data. He tentatively concluded that $c'_p \longrightarrow 0.4$ approximately as $\frac{hu_\tau}{\nu_s} \longrightarrow \infty$ for Mach numbers from 1.5 to 3.1. However, as shown in figure 11, the thick boundary-layer data of the present study do not support this conclusion; instead, they indicate a maximum value of 0.25 or less.

Hastings obtained the data band shown in figure 12 by plotting c'_p/c_f as a function of $\frac{hu_\tau}{\nu_s}$ for his thin boundary-layer data for Mach numbers of 1.56, 2.41, and 3.10. The thick boundary-layer flight data of the present study tend to agree with the data band. The local flow values, u_τ and ν_s, and the local skin friction values, c_f, were obtained for the present study from the boundary-layer rake data.[1] The data of the present study support Hastings' tentative conclusion that c'_p/c_f tends to a limit as $\frac{hu_\tau}{\nu_s}$ tends to infinity. In reference 6 he shows that the thin boundary-layer data of reference 4 also support this conclusion.

---

[1]The local skin friction coefficient was calculated from the rake data using the Clauser type of determination. Two other methods, a Preston probe and a skin friction balance, were also used to obtain local skin friction values. The values found with the three methods were in good agreement. Reference 16 presents a detailed discussion of the local skin friction coefficient and other boundary-layer characteristics.

The second generalized method was obtained from reference 10. This method is based on the concept that for any given Mach number there is a consistent relationship between the base pressure ratio, the Reynolds number, and the step height. For each of the Mach numbers of 1.5, 2.0, and 3.1, Chapman, Wimbrow, and Kester (ref. 4) established the dependence of the base pressure ratio on Reynolds number, step height, and distance from the leading edge. The resulting curves were fairly linear for each Mach number. In reference 10 the data from reference 4 as well as data from the X-15 aircraft (refs. 5 and 10) were used to obtain an average slope for the three base pressure ratios versus $\dfrac{c}{2hR^{1/5}}$ curves for Mach numbers of 1.5, 2.0, and 3.1. Then, by using the Mach-number-dependent variable k (fig. 13), which is a linearizing factor obtained in reference 10 from the data of references 4, 5, and 10, the data band in figure 14 was obtained. The band is based on data from several references, including references 3 to 7 and 10. All represent turbulent, thin boundary-layer flow. The flight data of the present study tend to agree with this data band.

The third generalized method is from reference 3. This method is based on the concept that there is a limiting base pressure coefficient for a given Mach number as h/θ approaches infinity. In practice, as stated by Nash (ref. 3), the variation of the correlation parameter $(c_{p,b})_1$ with Mach number is chosen to give the best correlation. The values chosen by Nash are, in effect, a most negative limit for the turbulent flow viscous base pressure data he studied. Nash's variation of $(c_{p,b})_1$ for Mach numbers of interest to the present study are:

M	$(c_{p,b})_1$
1.4	-0.390
1.6	-.326
1.8	-.285
2.0	-.252
2.2	-.224
2.4	-.200
2.6	-.178

The curve shown in figure 15 from reference 3 was obtained from thin boundary-layer flight and wind-tunnel data for Mach numbers primarily between 1.5 and 3.1. The thick boundary-layer data of the present study for Mach numbers near 1.5 are close to the correlation curve. However, for a Mach number of 2.0 the curve from reference 3 underestimates the drag derived from the aft-facing step in flight, and at $M = 2.4$ the discrepancy (underestimation) is even greater.

Effects of Aft-Facing Steps on Supersonic Operations

Predictions of the drag penalty associated with aft-facing discontinuities (up to 2.54 millimeters (0.1 inch)) at cruise conditions for a hypothetical supersonic transport are presented in reference 22 for two distances from the leading edge, 3.0 meters (10 feet) and 30.5 meters (100 feet). The drag penalty for 30.5 linear meters (100 linear feet) of step was calculated for a hypothetical supersonic transport cruising at a Mach number of 2.7 and an altitude of 19.8 kilometers (65,000 feet) with a lift-to-drag ratio of 8.5 and a cruise weight of 1668 kilonewtons (375,000 pounds). The predicted curves from reference 22 and drag penalty data for the 1.42-centimeter (0.56-inch) step height of this study (15.9 meters (52.1 feet) from the leading edge) are shown in figure 16. The point for the present study was derived by extrapolating the base pressure coefficient data from a Mach number of 2.5 to 2.7. The point for reference 6 was derived by using the base pressure coefficient data from the 2.41 and 3.10 Mach numbers for θ/h values near those of the present study and by assuming a step height of 1.42 centimeters (0.56 inch). A curve (dashed) for a chord length of 15.9 meters (52.1 feet) from the leading edge was determined by using the point from the data of the present study and the two curves from reference 22. For a supersonic transport with a 4800-kilometer (3000-mile) cruise range, assuming initial cruise weight to be 1917 kilonewtons (431,000 pounds) and final cruise weight to be 1410 kilonewtons (317,000 pounds), a 0.68-percent increase in drag causes approximately 3114 newtons (700 pounds) more fuel to be burned (or the payload to be decreased by that amount). Thus, step discontinuities do have enough effect on the drag of large supersonic aircraft to justify the development of better methods of predicting their effects on range and payload.

CONCLUSIONS

Thick boundary-layer aft-facing step data obtained from flights of an XB-70 airplane were analyzed for Mach numbers from 0.4 to 2.5 and compared with semi-empirical estimates and thin boundary-layer wind-tunnel results. The analysis showed that:

(1) The lower pressures on the base of the step were propagated farther forward of the step in a thick boundary layer than in a thin boundary layer.

(2) The base pressure ratio was lower for ratios of momentum thickness to step height near 1 for Mach numbers of approximately 2.0 and 2.4 than indicated by the corresponding small-scale wind-tunnel data or semiempirical estimates. Hence, the present flight data showed more drag than would have been predicted.

(3) The subsonic flight base pressure coefficients were in good agreement with the coefficients found with Hoerner's semiempirical method, which used the ratio of momentum thickness to step height to account for effects of boundary-layer thickness.

(4) The base pressure coefficient for thick boundary layers did not have the abrupt peak near a Mach number of 1.1 exhibited by thin boundary-layer data from the wind tunnel. Instead, it gradually reached a maximum value between Mach

12

numbers of 1.3 and 1.5 before beginning the decrease that is characteristic of supersonic flow.

(5) The present data tended to agree with the data bands of both a general method which used a pressure recovery coefficient for a correlating parameter and a general method which used a Mach-number-dependent factor for a correlating parameter. The present flight data for Mach numbers near 1.5 were in good agreement with the results of a general method which used the limiting base pressure coefficient as a correlating parameter, but flight data for Mach numbers near 2.0 and 2.4 did not agree with the results of this method.

(6) A 0.68-percent drag penalty at cruise conditions was shown to result from 30.5 linear meters (100 linear feet) of a 1.42-centimeter (0.56-inch) aft-facing step located 15.9 meters (52.1 feet) from the wing leading edge of a hypothetical supersonic transport.

Flight Research Center
 National Aeronautics and Space Administration
  Edwards, Calif., January 12, 1973

REFERENCES

1. Saltzman, Edwin J.; Goecke, Sheryll A.; and Pembo, Chris: Base Pressure Measurements on the XB-70 Airplane at Mach Numbers From 0.4 to 3.0. NASA TM X-1612, 1968.

2. Korst, H. H.: A Theory for Base Pressures in Transonic and Supersonic Flow. J. Appl. Mech., vol. 23, no. 4, Dec. 1956, pp. 593-600.

3. Nash, J. F.: A Discussion of Two-Dimensional Turbulent Base Flows. NPL Aero Rep. 1162, British A.R.C., July 20, 1965.

4. Chapman, Dean R.; Wimbrow, William R.; and Kester, Robert H.: Experimental Investigation of Base Pressure on Blunt-Trailing-Edge Wings at Supersonic Velocities. NACA Rept. 1109, 1952. (Supersedes NASA TN 2611.)

5. Saltzman, Edwin J.: Base Pressure Coefficients Obtained From the X-15 Airplane for Mach Numbers Up to 6. NASA TN D-2420, 1964.

6. Hastings, R. C.: Turbulent Flow Past Two-Dimensional Bases in Supersonic Streams. R. & M. No. 3401, British A.R.C., 1965.

7. Hama, Francis R.: Experimental Investigations of Wedge Base Pressure and Lip Shock. JPL Tech. Rep. 32-1033, Jet Prop. Lab., Dec. 1, 1966.

8. Nash, J. F.; Quincey, V. G.; and Callinan, J.: Experiments on Two-Dimensional Base Flow at Subsonic and Transonic Speeds. NPL Aero Rep. 1070, British A.R.C., Jan. 21, 1963.

9. Sfeir, Abdallah: Supersonic Flow Separation on a Backward Facing Step. Rept. no. AS-66-18 (AFOSR 67-0656, DDC No. AD 647958), Div. of Aeron. Sciences, Univ. of Calif. at Berkeley, Dec. 1966.

10. Goecke, Sheryll A.: Comparison of Wind-Tunnel and Flight-Measured Base Pressures From the Sharp-Leading-Edge Upper Vertical Fin of the X-15 Airplane for Turbulent Flow at Mach Numbers From 1.5 to 5.0. NASA TN D-6348, 1971.

11. Nash, J. F.: An Analysis of Two-Dimensional Turbulent Base Flow, Including the Effect of the Approaching Boundary Layer. NPL Aero Rep. 1036, British A.R.C., July 30, 1962.

12. Saltzman, Edwin J.; and Bellman, Donald R.: A Comparison of Some Aerodynamic Drag Factors as Determined in Full-Scale Flight With Wind-Tunnel and Theoretical Results. Facilities and Techniques for Aerodynamic Testing at Transonic Speeds and High Reynolds Number, AGARD-CP-83-71, Aug. 1971.

13. Mechtly, E. A.: The International System of Units – Physical Constants and Conversion Factors. NASA SP-7012, 1969.

14. Kordes, Eldon E.; and Love, Betty J.: Preliminary Evaluation of XB-70 Airplane Encounters With High-Altitude Turbulence. NASA TN D-4209, 1967.

15. Taillon, Norman V.: A Method for the Surface Installation and Fairing of Static-Pressure Orifices on a Large Supersonic-Cruise Airplane. NASA TM X-1530, 1968.

16. Fisher, David F.; and Saltzman, Edwin J.: Local Skin Friction Coefficients and Boundary-Layer Profiles Obtained in Flight From the XB-70-1 Airplane at Mach Numbers Up to 2.5. NASA TN D-7220, 1973.

17. Webb, Lannie D.; and Washington, Harold P.: Flight Calibration of Compensated and Uncompensated Pitot-Static Airspeed Probes and Application of the Probes to Supersonic Cruise Vehicles. NASA TN D-6827, 1972.

18. Beers, Yardley: Introduction to the Theory of Error. Second ed., Addison-Wesley Publishing Co., Inc., 1962.

19. Carpenter, P. W.; and Tabakoff, W.: Survey and Evaluation of Supersonic Base Flow Theories. NASA CR-97129, 1968.

20. Chang, Paul K.: Separation of Flow. Pergamon Press Inc., 1970.

21. Hoerner, Sighard F.: Fluid-Dynamic Drag. Publ. by the author (148 Busteed Dr., Midland Park, N. J.), 1965.

22. Peterson, John B., Jr.; and Braslow, Albert L.: Implications of the Effects of Surface Temperature and Imperfections on Supersonic Operations. Conference on Aircraft Operating Problems, NASA SP-83, 1965, pp. 227-233.
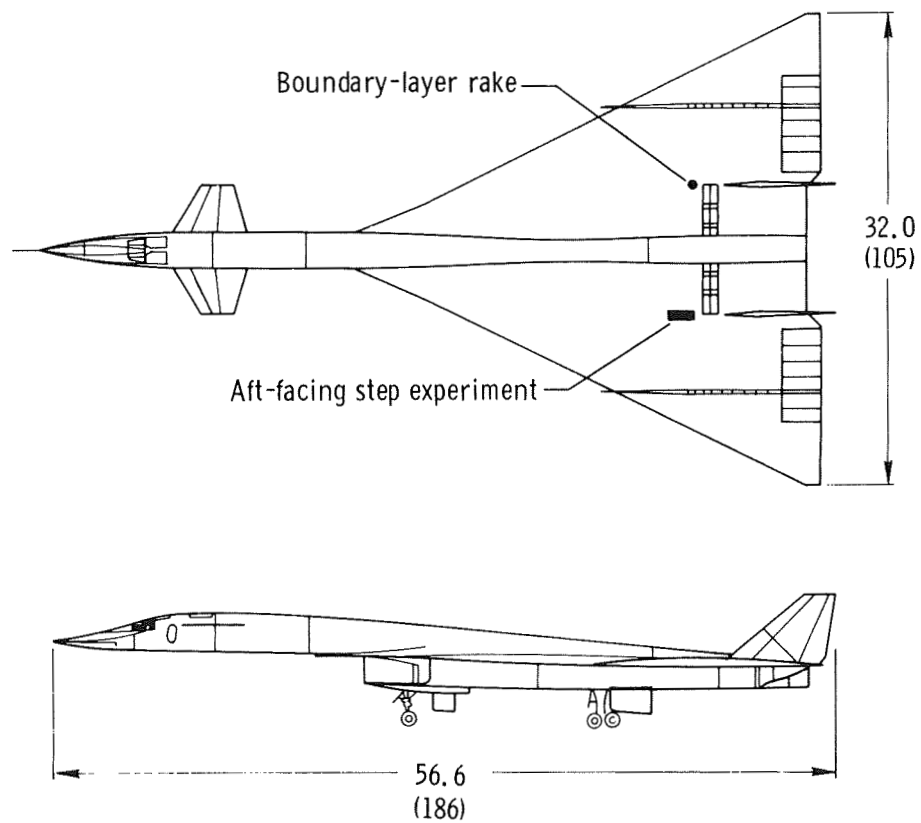
Figure 1. Two-view drawing of the XB-70 airplane showing location of the experiment. Length of run to step, 15.9 m (52.1 ft). Dimensions are in meters (feet).
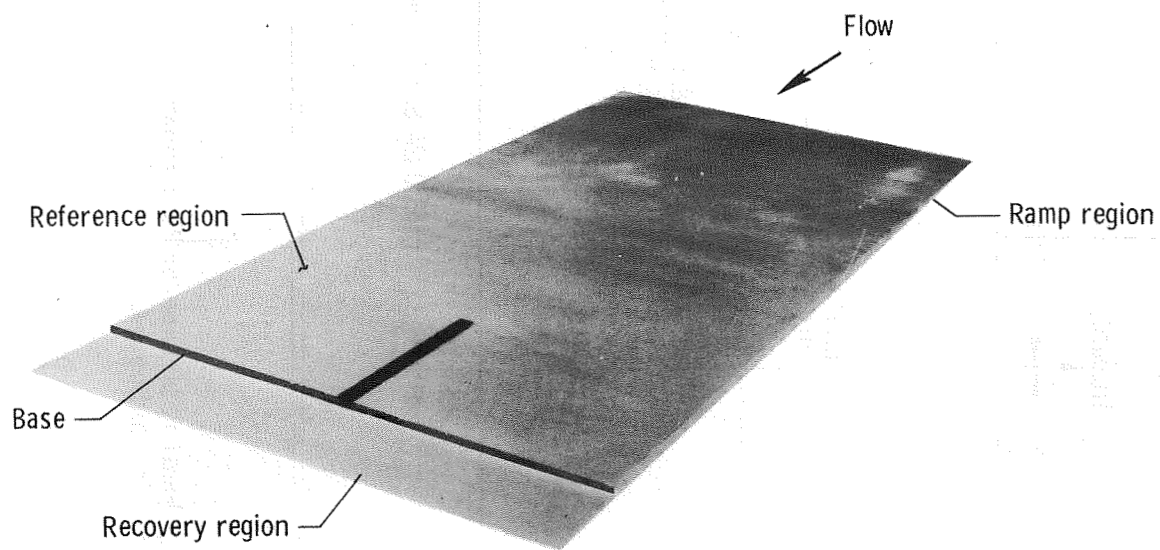
(a) Overall view.

Figure 2. Photograph and sketch of the aft-facing step experiment.
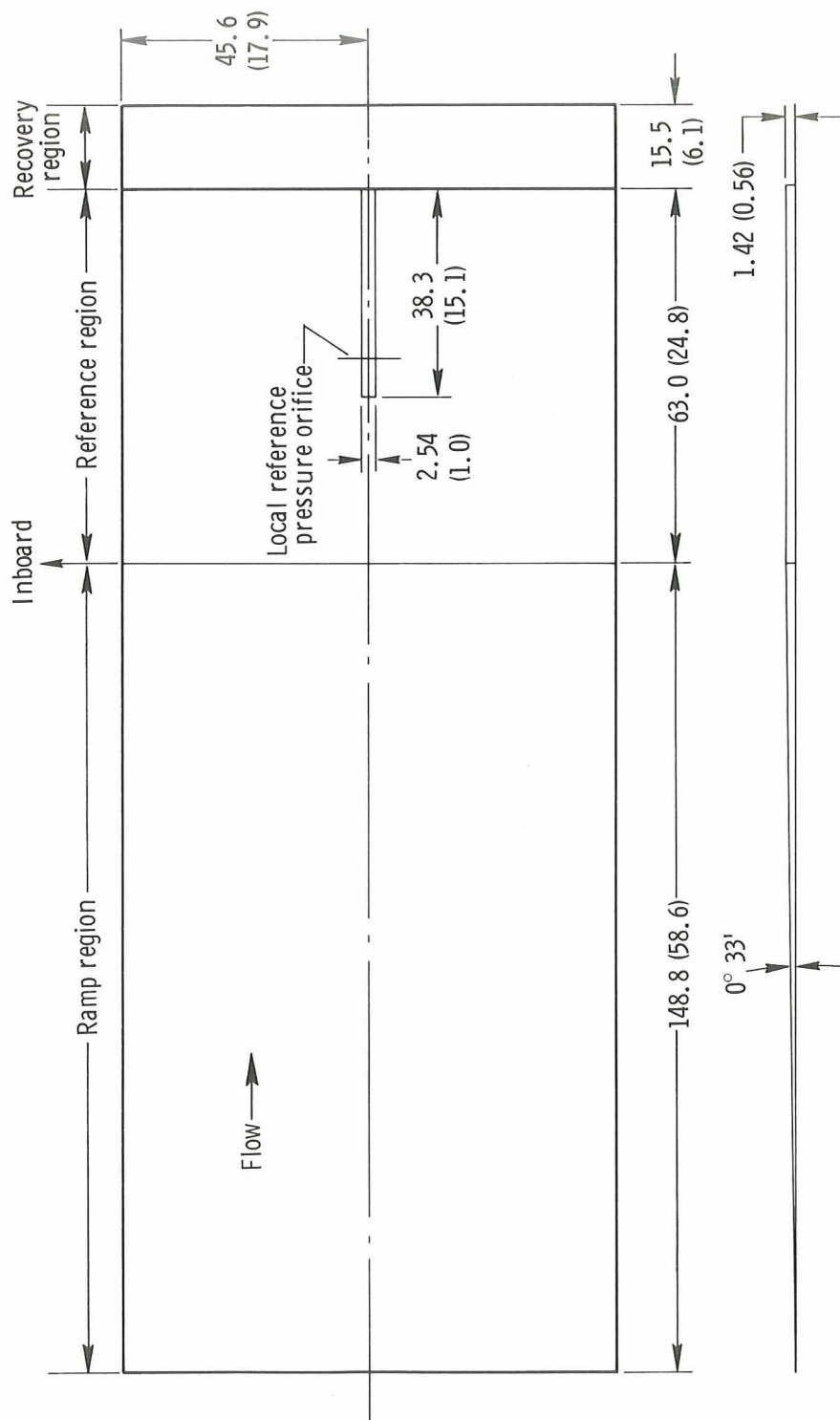
(b) Sketch showing general dimensions. Only local reference orifice shown. Dimensions are in centimeters (inches) except where otherwise indicated.

Figure 2. Concluded.
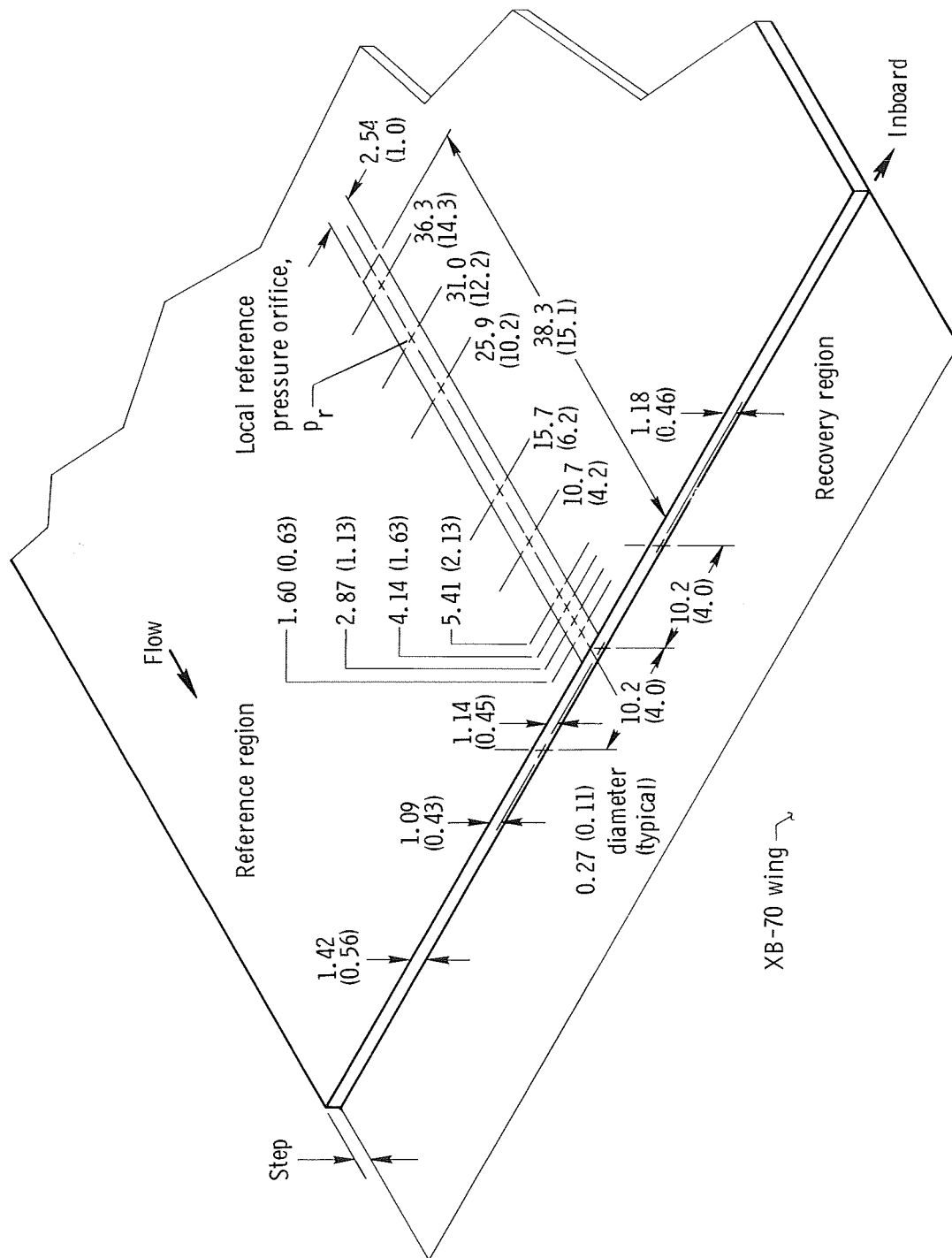
Figure 3. Locations of the static-pressure orifices in front of and on the aft-facing step. Dimensions refer to distances from step edge or step centerline and are in centimeters (inches).

19
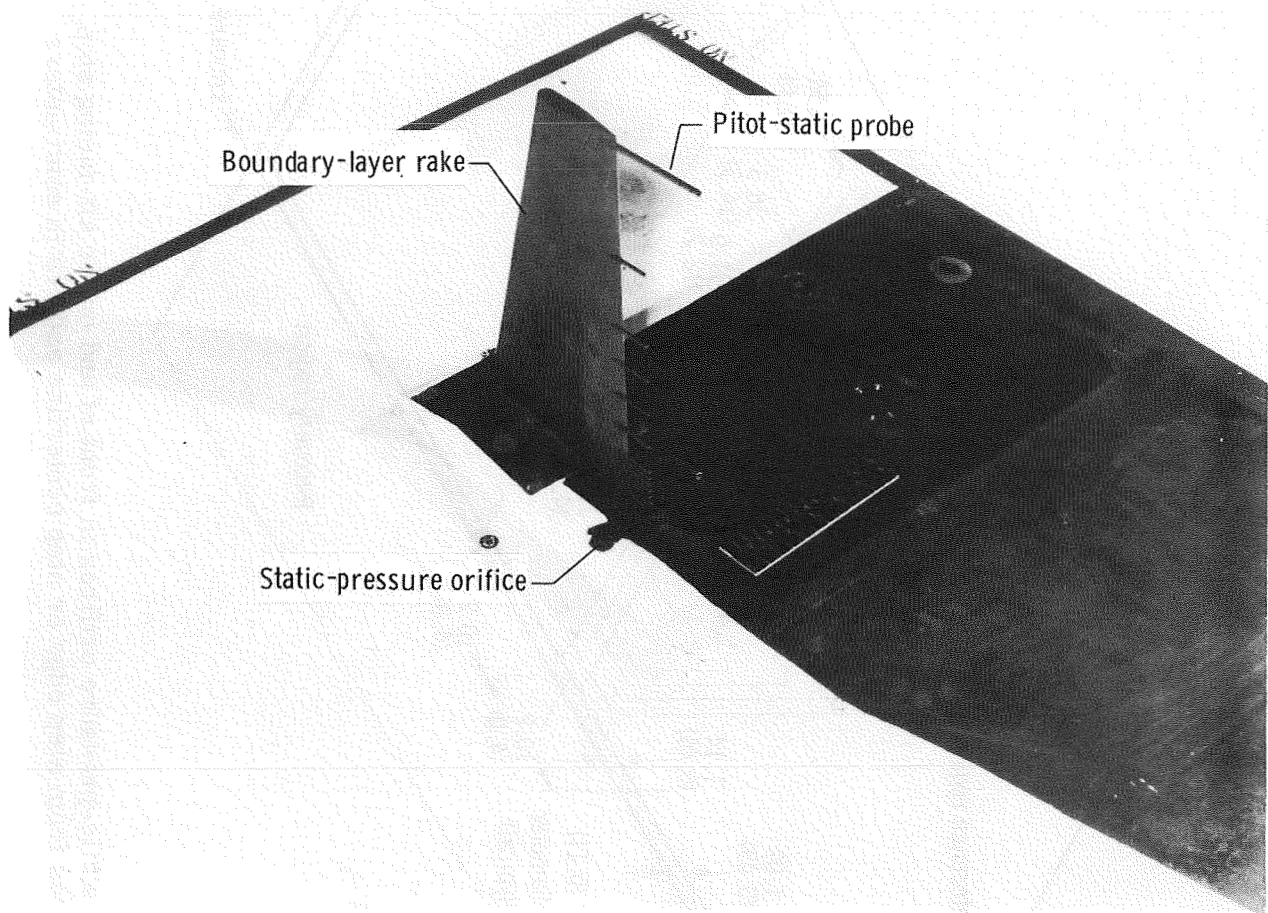
Figure 4. Photograph of the boundary-layer rake mounted on the upper surface of the right wing.
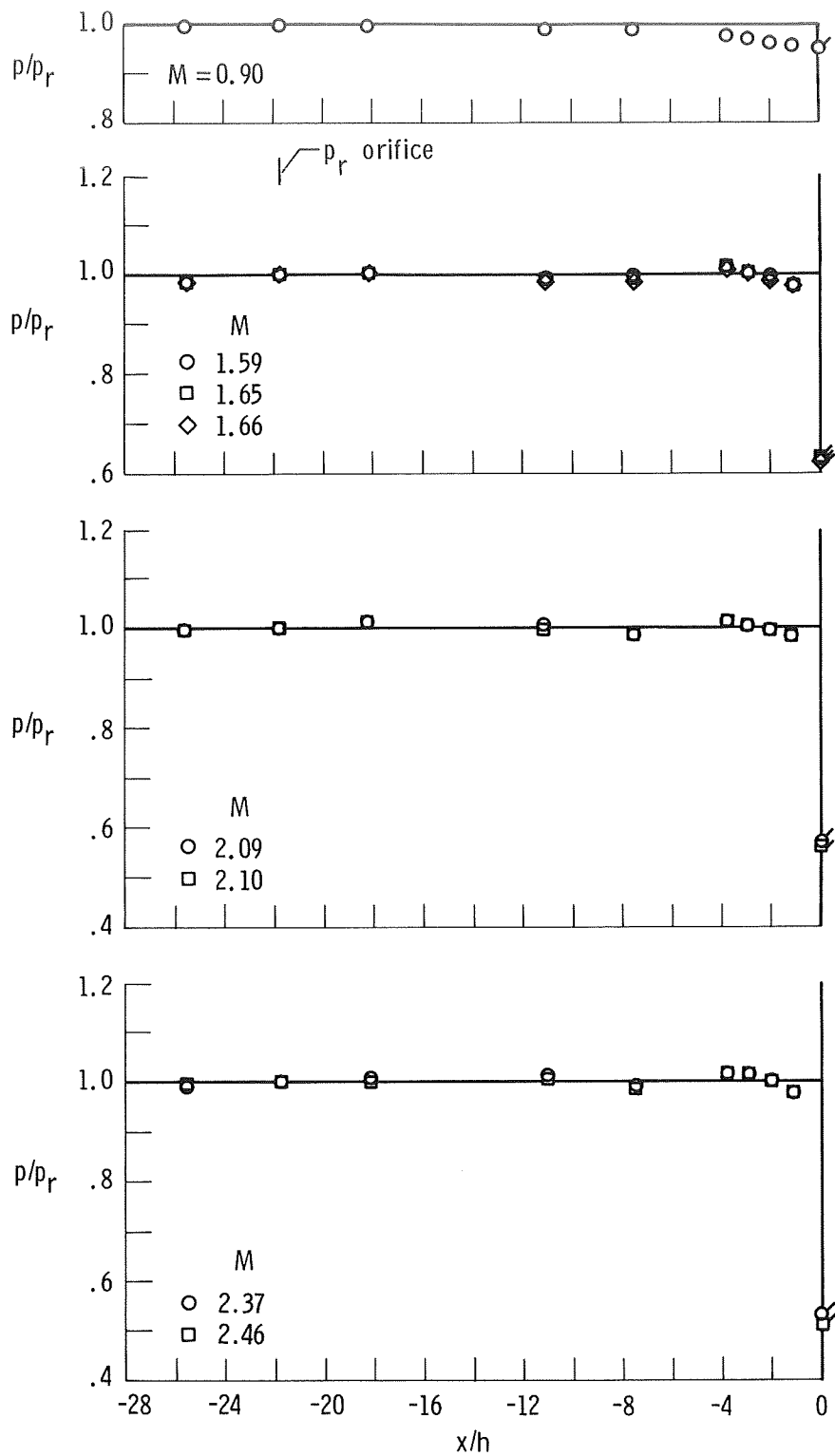
Figure 5. Pressure ratio profile along centerline of reference region as a function of distance upstream of step for turbulent flow. Flagged symbols represent base pressure ratio.
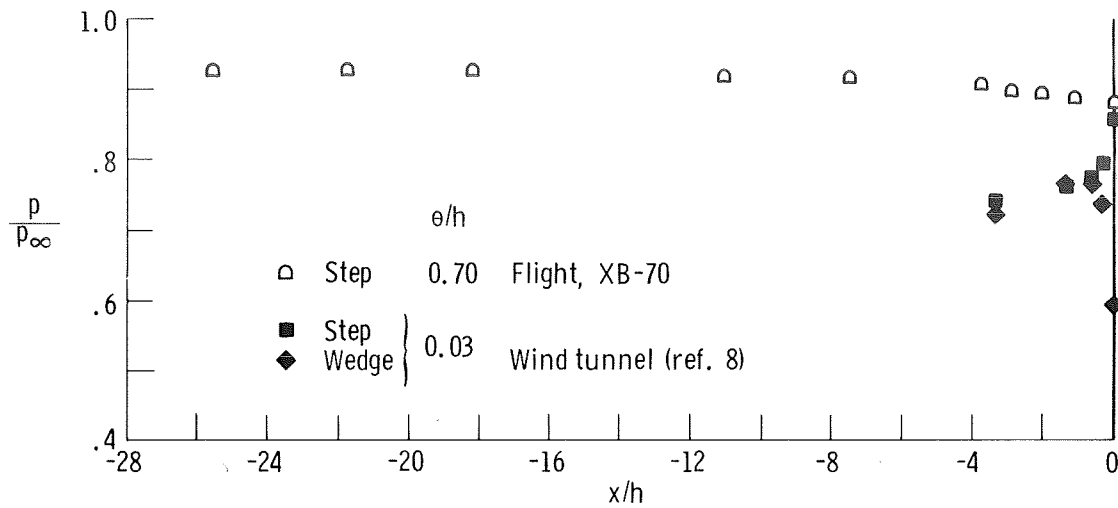
(a) M = 0.90.
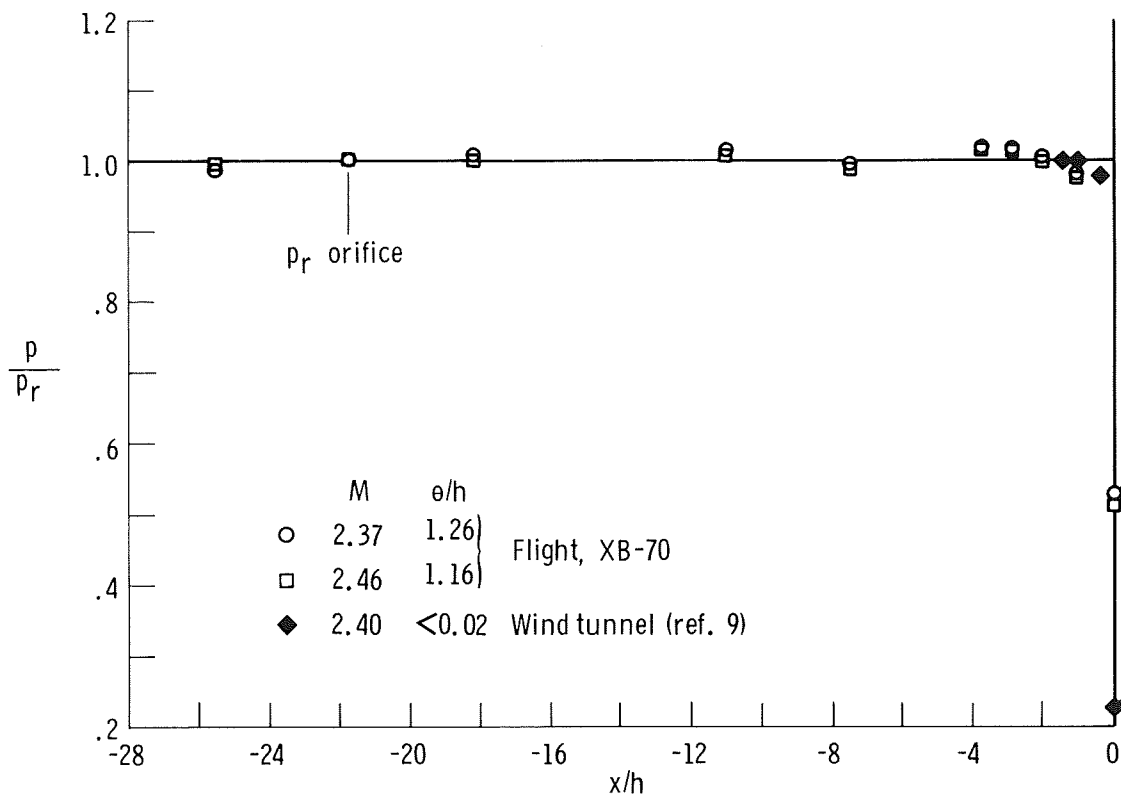
(b) M ≈ 2.40.

Figure 6. Comparison of flight-measured base pressure ratios and pressure profiles in front of the step with wind-tunnel data for turbulent flow. Flagged symbols represent base pressure ratio.
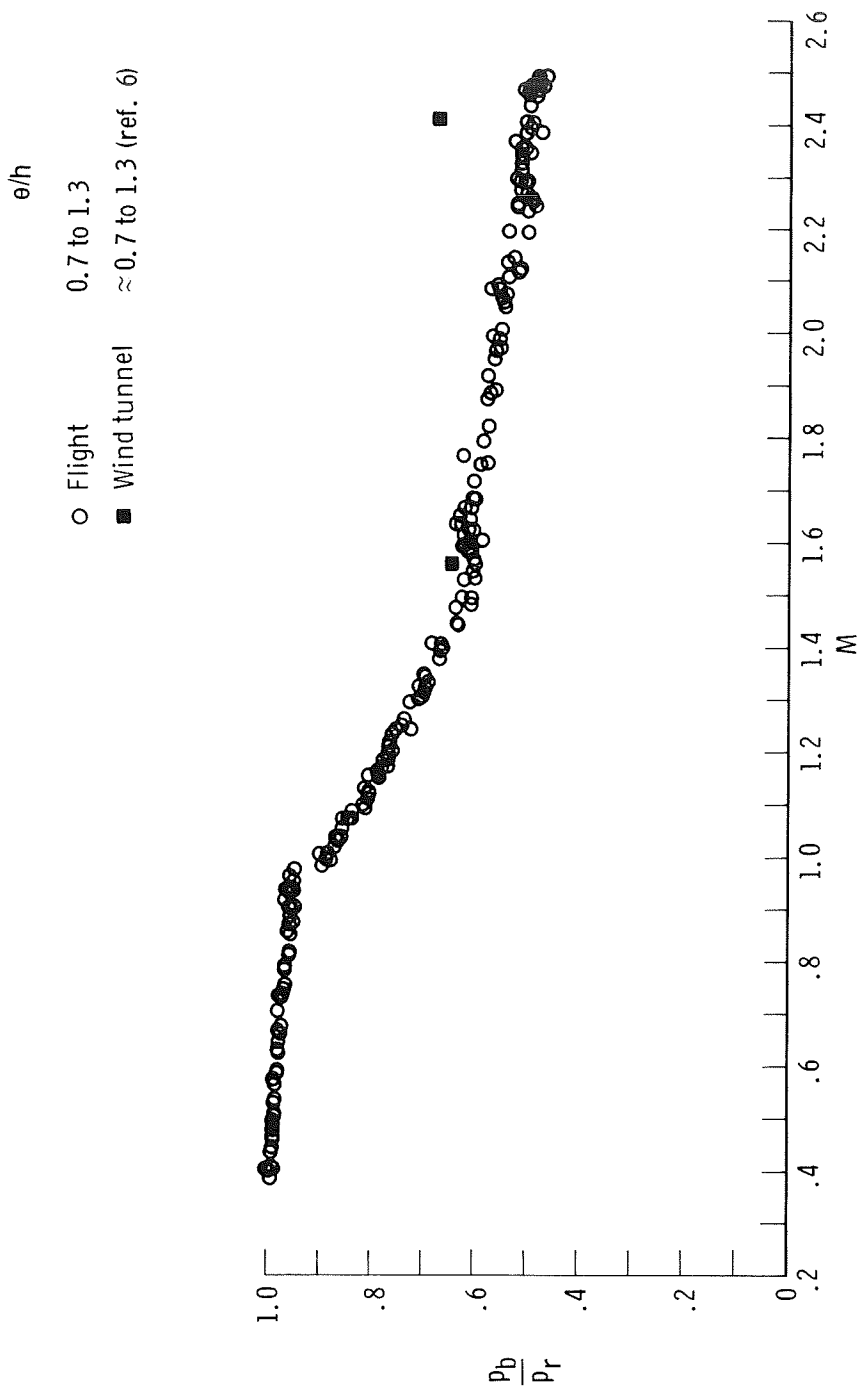
Figure 7. Flight base pressure ratio as a function of Mach number compared with wind-tunnel data for similar ratios of θ/h for turbulent flow.
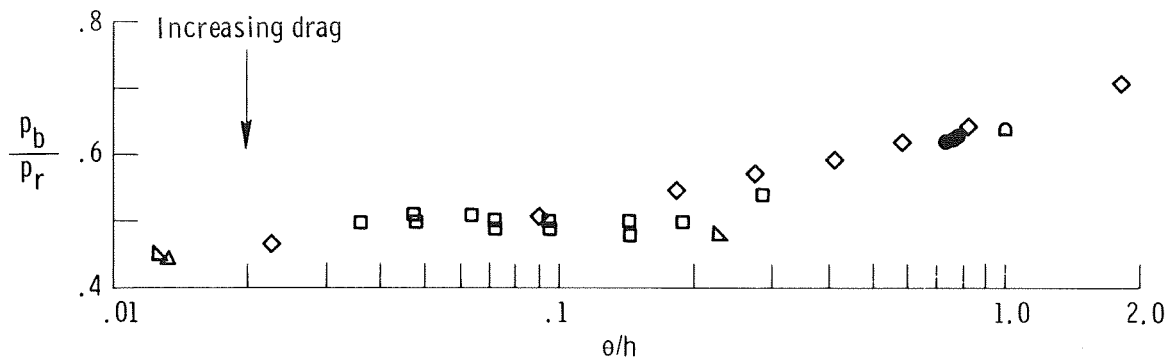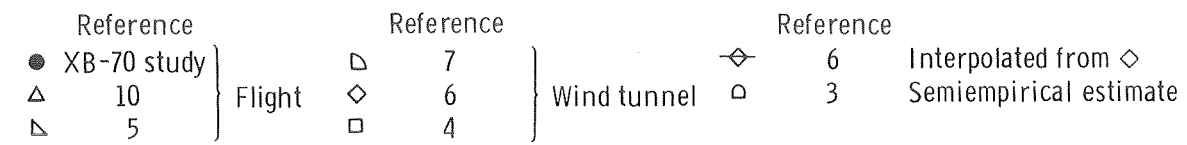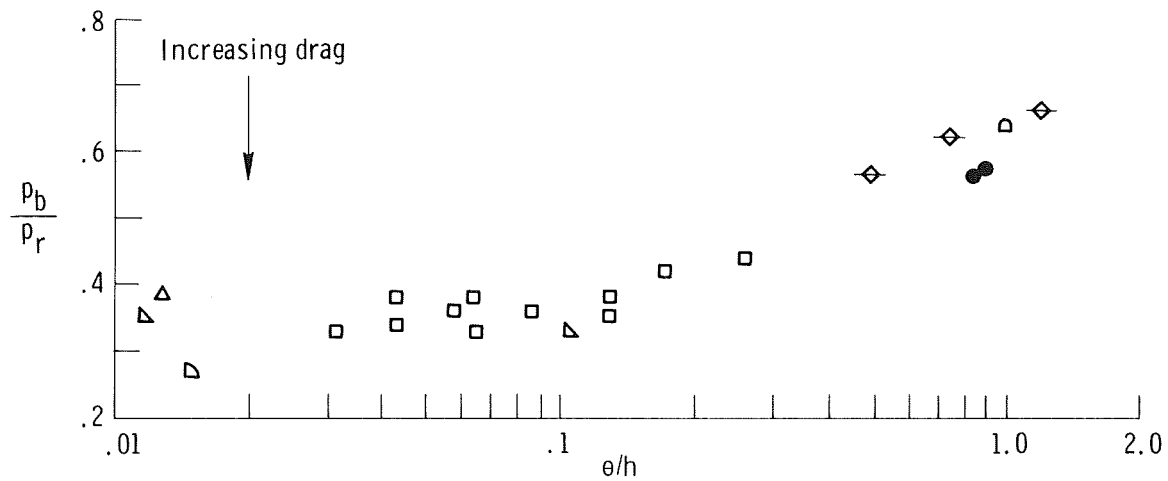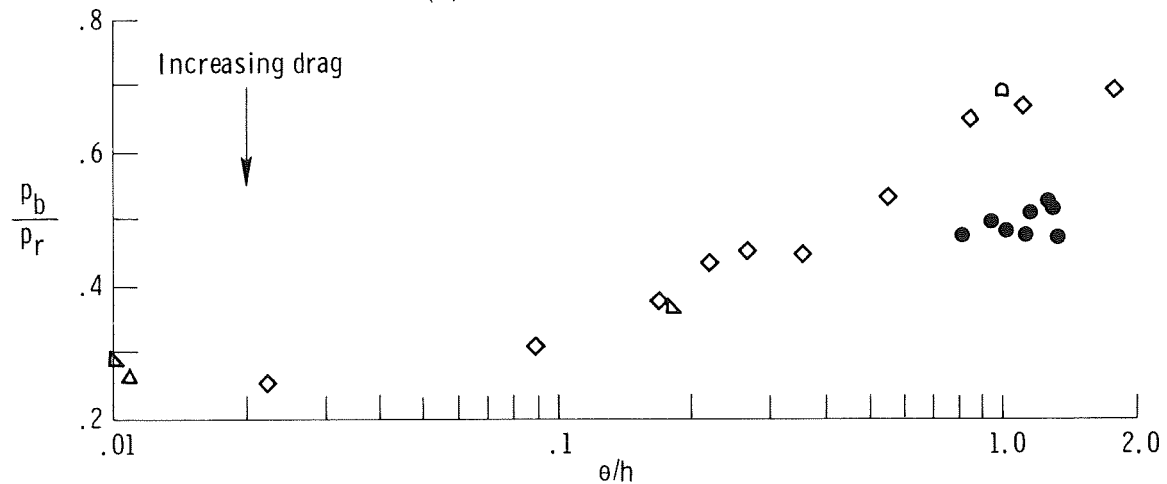
Figure 8. Base pressure ratio as a function of momentum thickness and step height for turbulent flow.
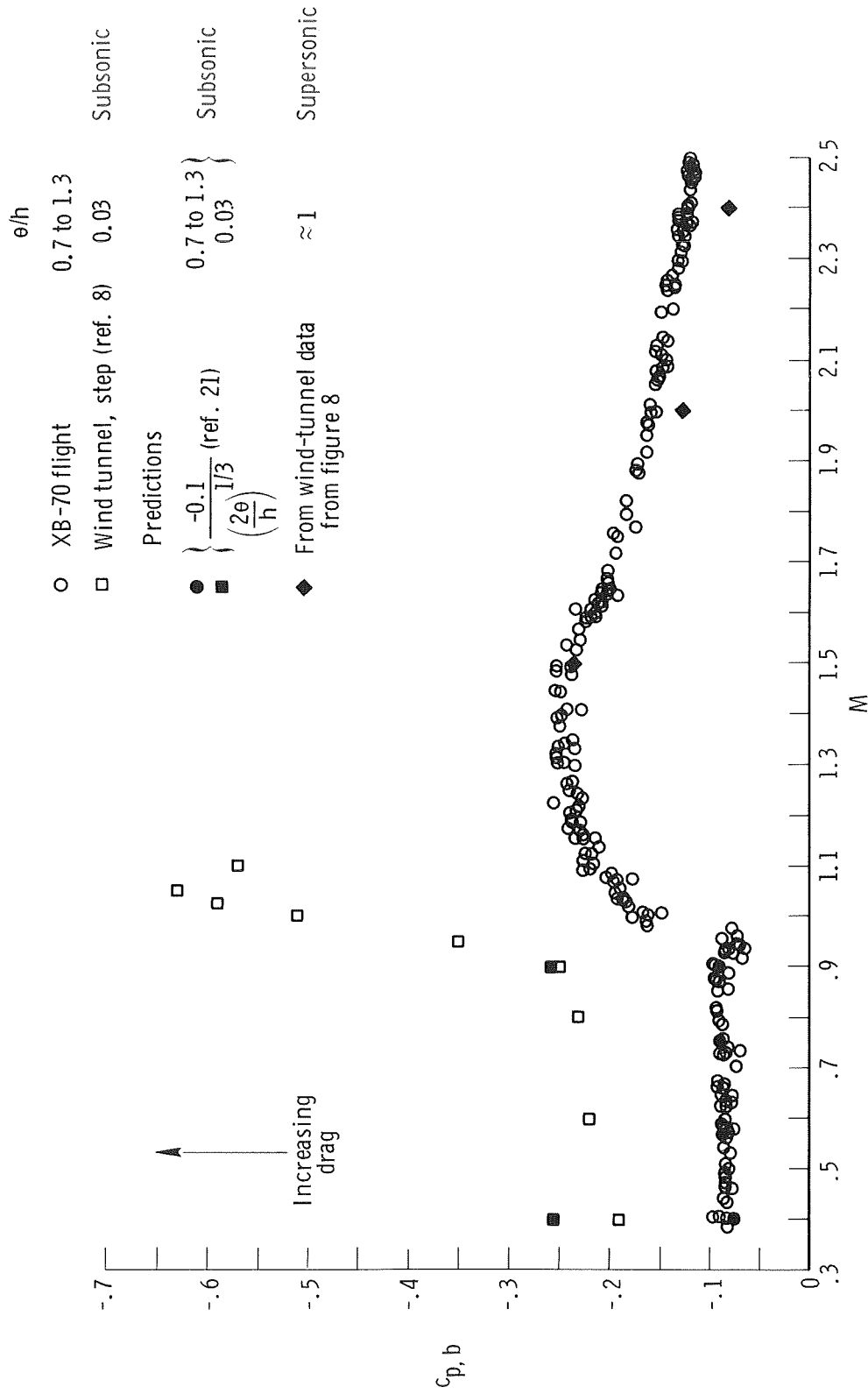
Figure 9. Comparison of flight-measured base pressure coefficients as a function of Mach number with wind-tunnel data and semiempirical predictions for turbulent flow.
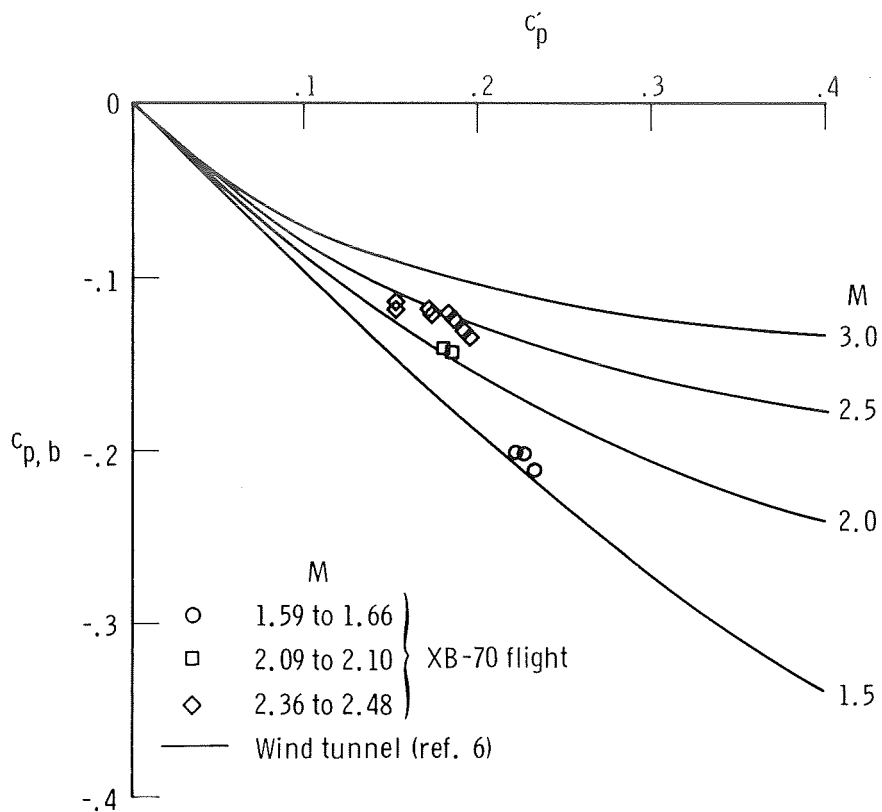
Figure 10. Variation of base pressure coefficient with pressure recovery coefficient.
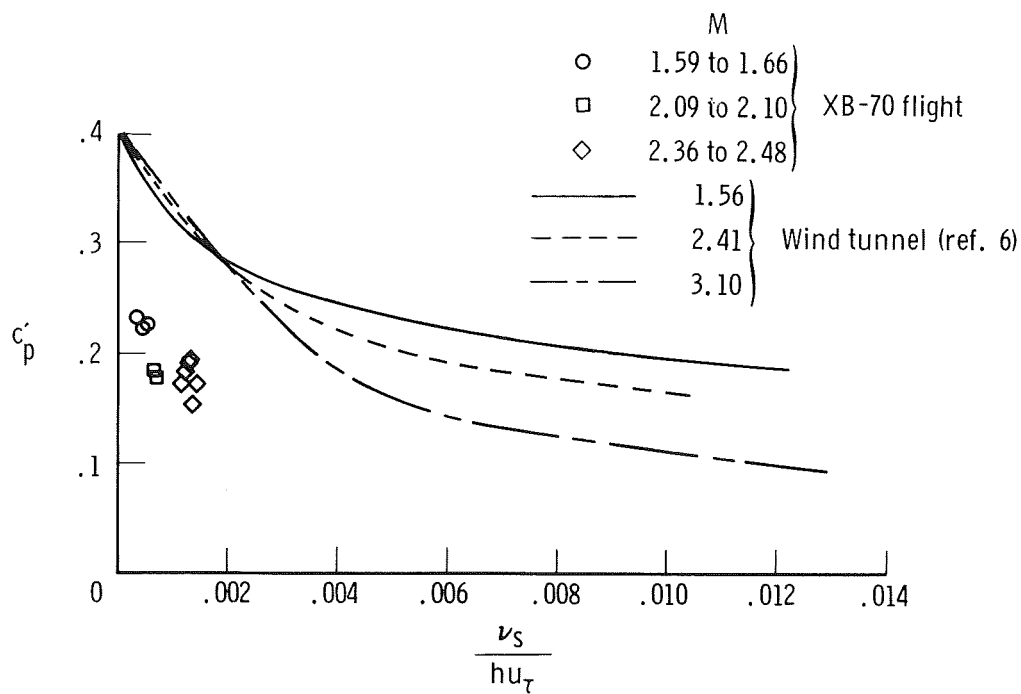
Figure 11. Variation of pressure recovery coefficient with ν_s/hu_τ.
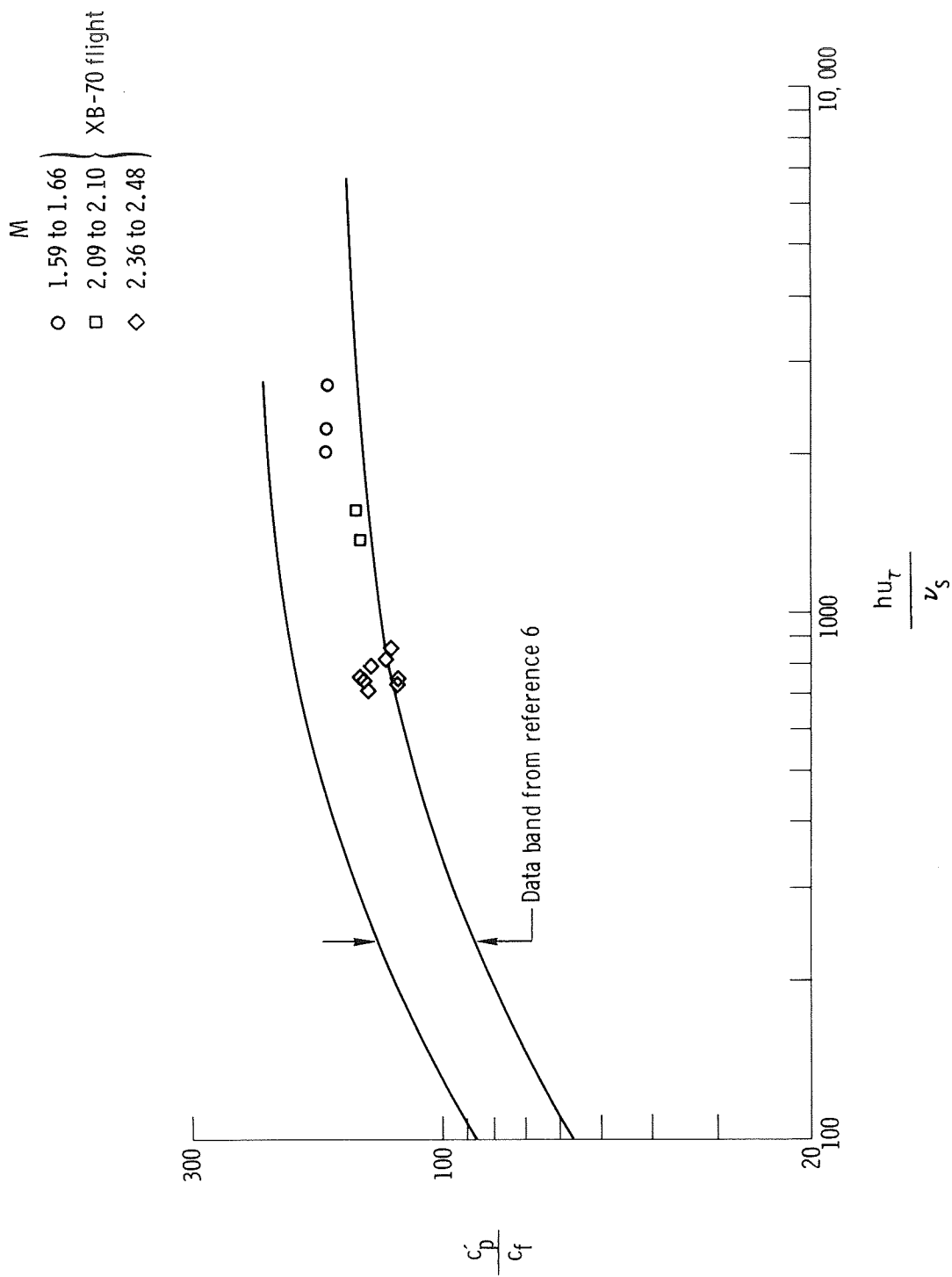
Figure 12. Comparison of the ratio c'_p/c_f of the present study as a function of hu_τ/ν_s with data band from reference 6 for turbulent flow.
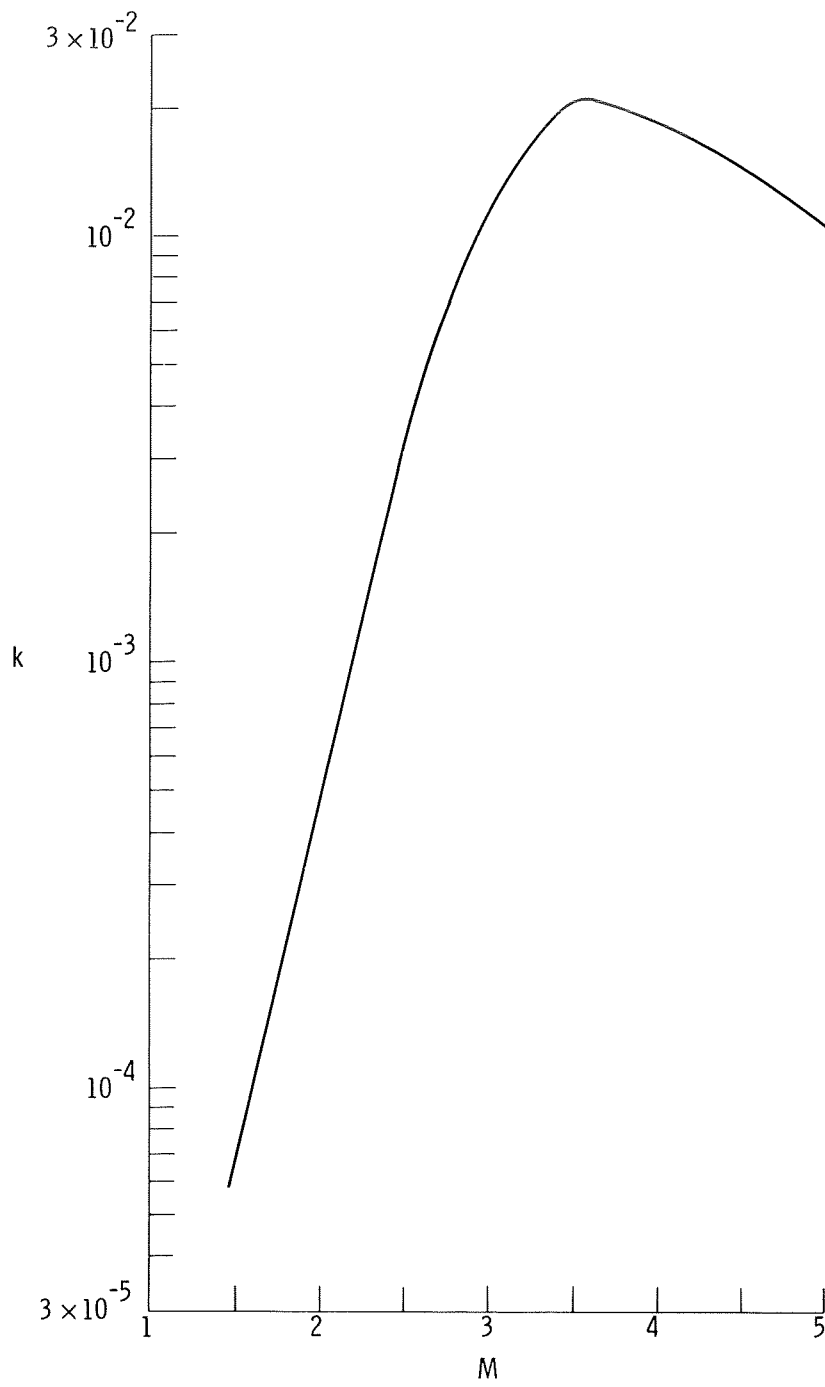
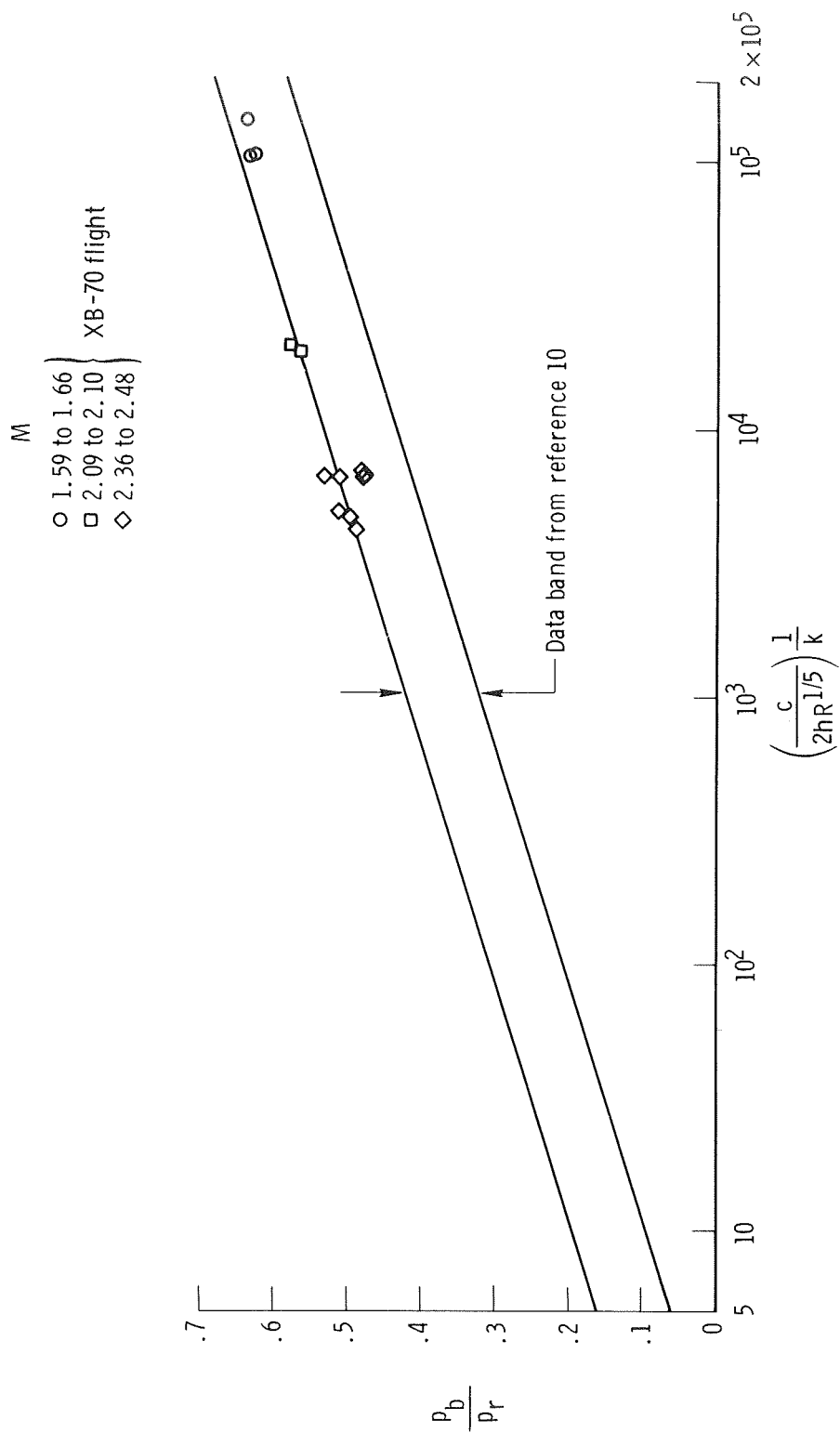Figure 13. Mach-number-dependent factor k as a function of Mach number (from ref. 10).

Figure 14. Comparison of the base pressure ratio of the present study as a function of $\left(\dfrac{c}{2\,hR^{1/5}}\right)\dfrac{1}{k}$ for turbulent flow.
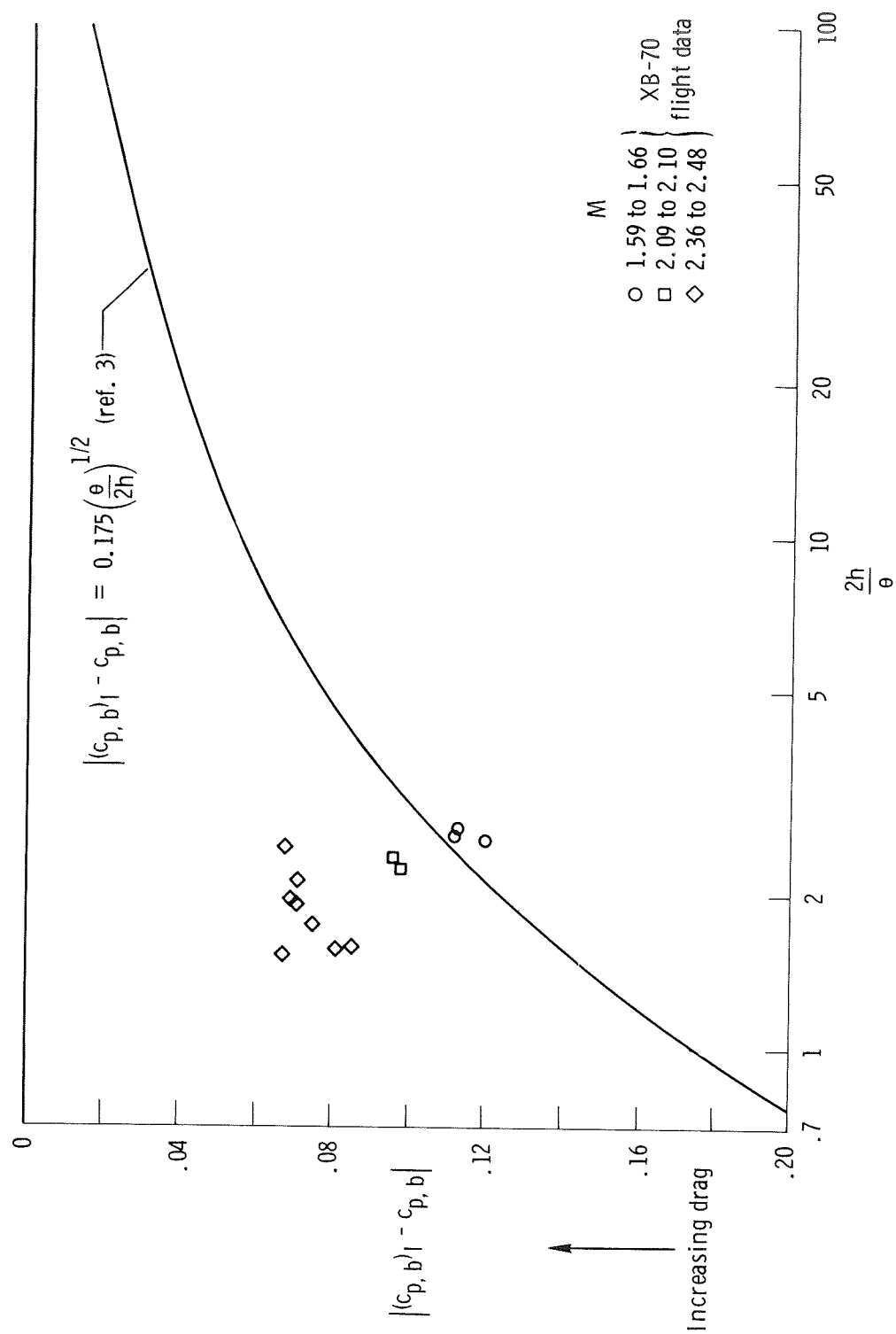
Figure 15. Comparison of the difference between the limiting base pressure coefficient and the base pressure coefficient of the present study with the curve from reference 3 for turbulent flow.
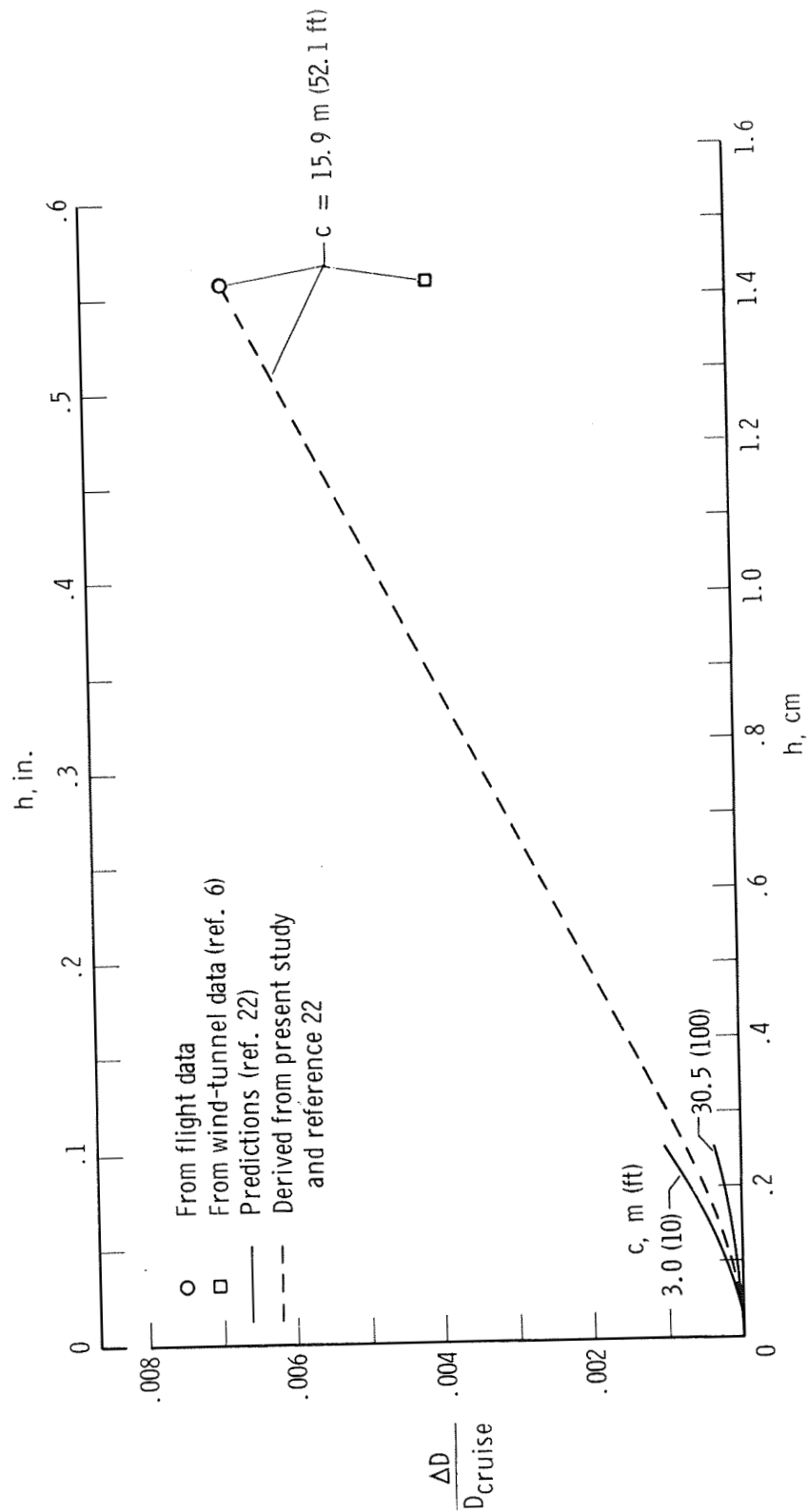
Figure 16. Drag penalty associated with 30.5 linear m (100 linear ft) of an aft-facing step on an aircraft cruising at Mach 2.7, an altitude of 19.8 km (65,000 ft), with a lift-to-drag ratio of 8.5, and a cruise weight of 1.668 kN (375,000 lb).

"The aeronautical and space activities of the United States shall be conducted so as to contribute . . . to the expansion of human knowledge of phenomena in the atmosphere and space. The Administration shall provide for the widest practicable and appropriate dissemination of information concerning its activities and the results thereof."
—NATIONAL AERONAUTICS AND SPACE ACT OF 1958

NASA SCIENTIFIC AND TECHNICAL PUBLICATIONS

TECHNICAL REPORTS: Scientific and technical information considered important, complete, and a lasting contribution to existing knowledge.

TECHNICAL NOTES: Information less broad in scope but nevertheless of importance as a contribution to existing knowledge.

TECHNICAL MEMORANDUMS: Information receiving limited distribution because of preliminary data, security classification, or other reasons. Also includes conference proceedings with either limited or unlimited distribution.

CONTRACTOR REPORTS: Scientific and technical information generated under a NASA contract or grant and considered an important contribution to existing knowledge.

TECHNICAL TRANSLATIONS: Information published in a foreign language considered to merit NASA distribution in English.

SPECIAL PUBLICATIONS: Information derived from or of value to NASA activities. Publications include final reports of major projects, monographs, data compilations, handbooks, sourcebooks, and special bibliographies.

TECHNOLOGY UTILIZATION PUBLICATIONS: Information on technology used by NASA that may be of particular interest in commercial and other non-aerospace applications. Publications include Tech Briefs, Technology Utilization Reports and Technology Surveys.

Details on the availability of these publications may be obtained from:

SCIENTIFIC AND TECHNICAL INFORMATION OFFICE

NATIONAL AERONAUTICS AND SPACE ADMINISTRATION

Washington, D.C. 20546